Salt Effect on Microstructures in Cationic Gemini Surfactant Solutions as Studied by Dynamic Light Scattering

Ting Lu,† Jianbin Huang,* and Dehai Liang*

Beijing National Laboratory for Molecular Science and College of Chemistry and Molecular Engineering, Peking University, Beijing 100871, P. R. China

Received September 12, 2007. In Final Form: November 6, 2007

A cationic gemini surfactant, dodecanediyl-1,12-bis(dodecyldiethylammonium bromide) ($C_{12}C_{12}C_{12}$(Et)), in aqueous solutions with varying NaBr concentration was studied by dynamic light scattering (DLS). As a comparison, its single-chained counterpart, dodecyl triethylammonium bromide (DTEAB), was also investigated under the same conditions. Similar to the case of a polyelectrolyte, $C_{12}C_{12}C_{12}$(Et) underwent a typical "ordinary-to-extraordinary (o−e) transition" with decreasing salt concentration to zero. At higher salt concentration, a single relaxation mode, corresponding to the diffusion of regular micelles, was observed. While in the "extraordinary regime", DLS detected two characteristic relaxation modes with the values of the diffusion coefficient being different by at least 2 orders. The fast mode was consistent with the polyion−small ion coupled-mode theories, as well as the direct polyion−polyion repulsion interactions. Because the slow mode disappeared at elevated salt concentrations and generated negligible scattered intensity, we attributed it to multimacroion domains.

Introduction

Gemini surfactants, typically formed from two monomeric surfactants linked by a spacer group at the level of the headgroups or very close to the headgroups, have attracted a great deal of attention over the past decades.[1−6] Compared with those of the conventional single-chain surfactants, gemini surfactants show many superior properties, especially in terms of extremely low critical micelle concentrations (cmc's) and low Krafft points.[5] Considerable effort has been made to design and synthesize new forms of gemini surfactants[7] as well as to investigate their aggregation behaviors by tuning the properties of the spacer, the headgroups, or the side chains.[8]

The most widely studied gemini surfactants were those derived from dicationic quaternary ammonium compounds, which could be abbreviated as $C_MC_SC_M$(Me), with *M* and *S* denoting the number of carbon atoms in the side alkyl chain and in the methylene spacer, respectively.[9,10] It has been reported that the spacer length or hydrophobicity showed a profound effect on the aggregation behavior.[9,11] Our studies also demonstrated that changing the methyl (Me) group in the headgroups to the ethyl (Et) group would enhance the aggregation capability of $C_{12}C_SC_{12}$ serials (S = 4, 6, 8, 10, 12) in aqueous solutions.[2] Besides hydrophobicity, salt concentration was demonstrated as another crucial factor affecting the aggregation of the gemini surfactants. Transmission electron microscopy (TEM) studies showed that the vesicles formed by $C_{12}C_SC_{12}$ serials (S = 4, 6, 8, 10, 12) in deionized water were transformed to micelles when induced by 0.02 mol/L NaBr.[2] Such phenomenon was not observed in their single-chained counterpart.

Upon forming gemini surfactants, the number of charges in the headgroup doubled, generating much stronger electrostatic interactions between the molecules. At a concentration above the cmc, micellar structures formed by gemini surfactants work as macroions and may exhibit similar behaviors as in the case of regular polyelectrolytes. Dynamic light scattering (DLS) studies have demonstrated that the structure and dynamics of polyelectrolytes were very sensitive to salt concentration and an "ordinary-to-extraordinary" transition occurred with decreasing ion strength to a certain level.[12−16] Above that level, a single diffusion coefficient, mainly representing that of the Brownian motion of an individual polymer chain, was obtained, which was considered as the "ordinary regime". While in the "extraordinary regime", two diffusion modes, bracketing the value expected for single chain diffusion, were measured by DLS. The fast mode could be reasonably explained by polyion−small ion couple-mode theories as well as direct polyion−polyion repulsion interactions.[12,16−18] Due to the longer interaction range of the electrostatic force, the fast-moving small ions generated a fluctuating electric filed. Therefore, the movement of the polyion was driven not only by the Brownian motion but also by the dragging force resulting from such electric field. Because the lower salt concentration weakened the screening of the polyion charge, the coupling became stronger and the diffusion speed

* To whom correspondence should be addressed. E-mail: dliang@pku.edu.cn (D.L.); JBHuang@pku.edu.cn (J.H.). Telephone and Fax: 86-10-62756170 (D.L.). Telephone: 86-10-62753557 (J.H.). Fax: 86-10-62751708 (J.H.).

† E-mail: lt_chem@pku.edu.cn.

(1) Bell, P. C.; Bergsma, M.; Dolbnya, I. P.; Bras, W.; Stuart, M. C. A.; Rowan, A. E.; Feiters, M. C.; Engberts, J. B. F. N. *J. Am. Chem. Soc.* **2003**, *125*, 1551.

(2) Lu, T.; Han, F.; Mao, G.; Lin, G.; Huang, J.; Huang, X.; Wang, Y.; Fu, H. *Langmuir* **2007**, *23*, 2932.

(3) Menger, F. M.; Littau, C. A. *J. Am. Chem. Soc.* **1993**, *115*, 10083.

(4) Muzzalupo, R.; Infante, M. R.; Perez, L.; Pinazo, A.; Marques, E. F.; Antonelli, M. L.; Strinati, C.; La Mesa, C. *Langmuir* **2007**, *23*, 5963.

(5) Rosen, M. J. *Chemtech* **1993**, *23*, 30.

(6) Zana, R. *J. Colloid Interface Sci.* **2002**, *248*, 203.

(7) FitzGerald, P. A.; Carr, M. W.; Davey, T. W.; Serelis, A. K.; Such, C. H.; Warr, G. G. *J. Colloid Interface Sci.* **2004**, *275*, 649.

(8) Menger, F. M.; Keiper, J. S. *Angew. Chem., Int. Ed* **2000**, *39*, 1907.

(9) Zana, R.; Benrraou, M.; Rueff, R. *Langmuir* **1991**, *7*, 1072.

(10) Danino, D.; Talmon, Y.; Zana, R. *Langmuir* **1995**, *11*, 1448.

(11) Li, Y.; Li, P.; Dong, C.; Wang, X.; Wang, Y.; Yan, H.; Thomas, R. K. *Langmuir* **2006**, *22*, 42.

(12) Lin, S.-C.; Lee, W. I.; Schurr, J. M. *Biopolymers* **1978**, *17*, 1041.

(13) Schmitz, K. S. *ACS Symp. Ser.* **1994**, *548* (Macro-ion Characterization), 1−22.

(14) Schmitz, K. S.; Lu, M.; Singh, N.; Ramsay, D. J. *Biopolymers* **1984**, *23*, 1637.

(15) Sedlák, M. *Langmuir* **1999**, *15*, 4045.

(16) Sedlák, M. *J. Chem. Phys.* **1996**, *105*, 10123.

(17) Tivant, P.; Turq, P.; Drifford, M.; Magdelenat, H.; Menez, R. *Biopolymers* **1983**, *22*, 643.

(18) Schmitz, K. S. *An Introduction to Dynamic Light Scattering by Macromolecules*; Academic Press: San Diego, CA, 1990.

10.1021/la702832v CCC: $40.75
Published on Web 01/18/2008

was increased. The explanation of slow mode has remained controversial. It could be interpreted as the dynamics of large aggregates or clusters.[19−22] Since the slow mode disappeared at higher salt concentration, it was believed that the origin of the domain dynamics was from charge interactions instead of hydrophobic aggregations.

To testify whether such "extraordinary regime" exists in the solution of charged gemini surfactants, we chose $C_{12}C_{12}C_{12}$(Et) as the example and studied its behavior in aqueous solution with zero salt concentration by DLS. As a comparison, the behavior of a single-chained surfactant, dodecyl triethylammonium bromide (DTEAB), in the same conditions was also investigated. The salt effect on the fast and slow mode was also studied by adding varying NaBr amounts into the system.

Experimental Section

Materials. NaBr (AR grade) was purchased from Beijing Chemical Co. and used after heating at 500 °C for 6 h. The cationic gemini surfactant dodecanediyl-1,12-bis(dodecyldiethylammonium bromide) ($[C_{12}H_{25}(CH_3CH_2)_2N(CH_2)_{12}N(CH_2CH_3)_2C_{12}H_{25}]Br_2$, abbreviated as $C_{12}C_{12}C_{12}$(Et)) and the conventional cationic quaternary ammonium surfactant dodecyl triethylammonium bromide (DTEAB) were synthesized according to the procedure reported elsewhere.[2] $C_{12}C_{12}C_{12}$(Et) and DTEAB solutions with or without NaBr were prepared at room temperature and filtered through a filter with 0.22 μm diameter (Millipore, MA) to remove the dusts. Milli-Q water (18.2 MΩ cm) was used throughout the experiments.

Dynamic Light Scattering (DLS). A commercialized spectrometer (Brookhaven Instruments Corporation, Holtsville, NY) equipped with a 100 mW solid-state laser (GXC-III, CNI, Changchun, China) operating at 532 nm was used to conduct DLS. Photon correlation measurements in the self-beating mode were carried out at scattering angles of 20°∼120° by using a BI-TurboCo digital correlator. The normalized first-order electric field time correlation function, $g^{(1)}(\tau)$, is related to the line width distribution $G(\Gamma)$ by

$$g^{(1)}(\tau) = \int_0^\infty G(\Gamma)\, e^{-\Gamma\tau}\, d\Gamma \quad (1)$$

with τ being the delay time. By using a Laplace inversion program, CONTIN,[23] the normalized distribution function of the characteristic line width $G(\Gamma)$ was obtained. The average line width, $\bar{\Gamma}$, was calculated according to $\bar{\Gamma} = \int \Gamma\, G(\Gamma)\, d\Gamma$. The polydispersity index, PDI, was defined as PDI $= \mu_2/\bar{\Gamma}^2$ with $\mu_2 = \int(\Gamma - \bar{\Gamma})^2\, G(\Gamma)\, d\Gamma$. $\bar{\Gamma}$ was a function of both C and the scattering angle (θ), which can be expressed as

$$\bar{\Gamma}/q^2 = D(1 + k_d C)[1 + f(R_g q)^2] \quad (2)$$

where $q = 4\pi n/\lambda \sin(\theta/2)$ with n, λ, D, k_d, and f being the solvent refractive index, the wavelength in vacuum, the translational diffusive coefficient, the diffusion second virial coefficient, and a dimensionless constant, respectively. D can be further converted into the hydrodynamic radius R_h by using the Stokes−Einstein equation:

$$D = k_B T/6\pi\eta R_h \quad (3)$$

where k_B, T, and η are the Boltzmann constant, the absolute temperature, and the viscosity of the solvent, respectively.

Surface Tension. Surface tension measurements were conducted using the drop volume method at 25.00 ± 0.01 °C. The critical micelle concentration (cmc) was determined by the cross point of the two lines before and after the cmc on the surface tension versus log C curve.

(19) Foerster, S.; Schmidt, M.; Antonietti, M. *Polymer* **1990**, *31*, 781.
(20) Schmitz, K. S. *Chem. Phys.* **1982**, *66*, 177.
(21) Groehn, F.; Antonietti, M. *Macromolecules* **2000**, *33*, 5938.
(22) Sedlák, M.; Konak, C.; Stepanek, P.; Jakes, J. *Polymer* **1987**, *28*, 873.
(23) Provencher, S. W. *Comput. Phys. Commun.* **1982**, *27*, 229.

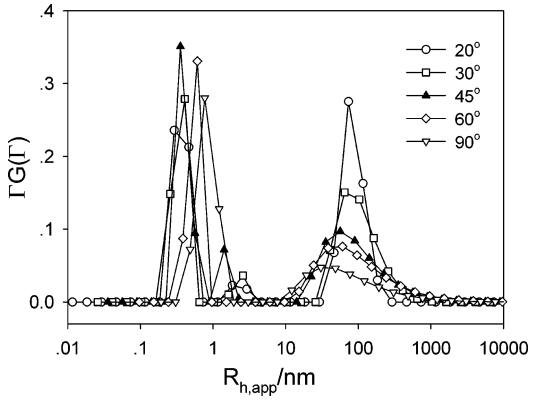

Figure 1. CONTIN analysis of $C_{12}C_{12}C_{12}$(Et) in aqueous solution without added salt, $C = 5$ mM.

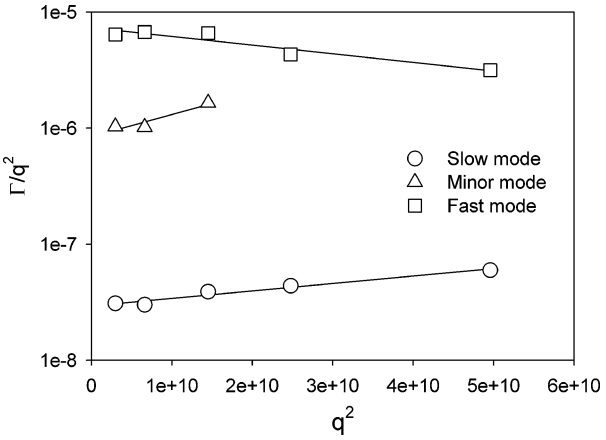

Figure 2. Angular dependence of the fast mode and slow mode shown in Figure 1.

Results and Discussion

Figure 1 shows the DLS results of $C_{12}C_{12}C_{12}$(Et) at 5.0 mM in deionized water at varying scattering angles at 25 °C. Two major components, both of which have a strong angular dependence, were observed in the system. The distribution of the component with a smaller size, corresponding to the fast mode, was relatively narrow at all the measured angles, while the distribution of the slow mode was broadened with increasing scattering angle. To compare their angular dependence, the plot of $\bar{\Gamma}/q^2$ versus q^2 (based on eq 2) was drawn in Figure 2. Clearly, the diffusion coefficients (D) of the two modes exhibited opposite trends with increasing scattering angle: the D value of the fast mode was decreased from 6.4×10^{-6} cm^2•s^{-1} at 20° to 3.1×10^{-6} cm^2•s^{-1} at 90°, while the D value of the slow mode increased from 3.0×10^{-8} cm^2•s^{-1} at 20° to 5.9×10^{-8} cm^2•s^{-1} at 90°. When extrapolating q^2 to zero, the D values of 2.8×10^{-8} and 7.0×10^{-6}cm^2•s^{-1}, which correspond to $R_{h,app}$ values of 87 and 0.35 nm, respectively, were obtained for the two modes. Considering the bond length of C−C was 0.154 nm, the fast mode with a $R_{h,app}$ value of 0.35 nm was too small to be the size of a single $C_{12}C_{12}C_{12}$(Et) molecule. The slow mode, whose size was about two orders higher, did not represent the single surfactant either. Moreover, based on eq 2, the $\bar{\Gamma}/q^2$ versus q^2 curve should exhibit no or very weak angular dependence when $R_g q \ll 1$. Obviously, the fast mode with the size of 0.35 nm does not follow this rule.

The effects of concentration and temperature on the bimodal distribution of $C_{12}C_{12}C_{12}$(Et) in aqueous solution with zero salt

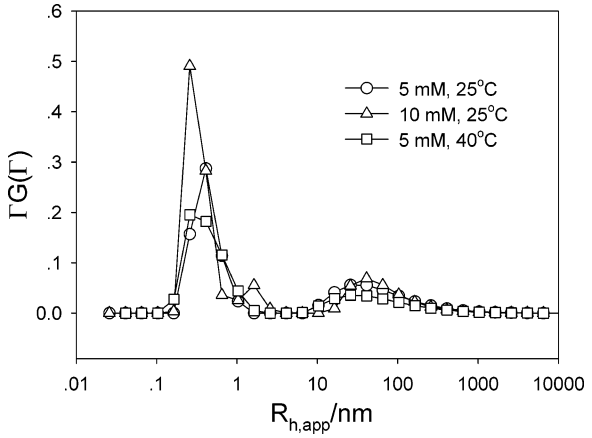

Figure 3. Concentration and temperature effect on the bimodal distribution of $C_{12}C_{12}C_{12}$(Et) solution without added salt.

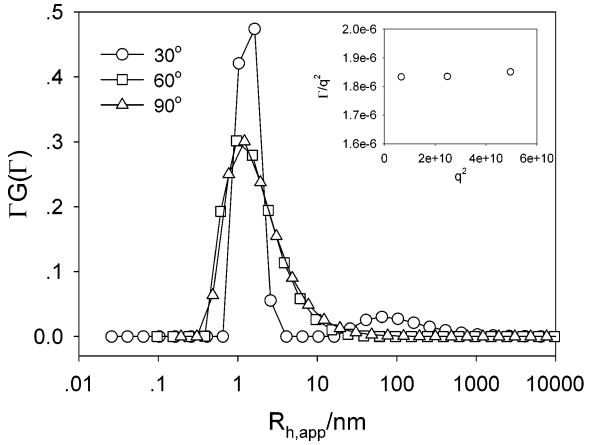

Figure 4. CONTIN analysis of DTEAB solution without added salt, $C = 20$ mM. The inset shows the angular dependence of the major component.

concentration were also investigated. It was found that both modes showed very weak concentration dependence, and their size and distribution remained even at 40 °C (Figure 3). Note that a minor diffusion mode was also observed in the system. As shown in Figures 1 and 3, it was frequently visualized at lower angles, higher concentrations, and lower temperatures. Figure 2 also demonstrates that the minor mode showed a very strong angular dependence. Considering that it was in between the two main peaks, and exhibited a very small area ratio, it was probably an artificial peak from the CONTIN program.

DTEAB, which is regarded as the monomer of the above-mentioned gemini surfactant, was also studied by DLS in aqueous solution without adding salt. Since the aggregation capability of DTEAB was much weaker than that of the gemini surfactant, a 4 times higher concentration (20 mM) was used in the study. As shown in Figure 4, a bimodal distribution with a much weaker slow mode was observed at 30°, and the slow mode was merged into the fast mode at higher scattering angles. The inset in Figure 4 also shows that the diffusion rate of the fast mode had almost no angular dependence and its value at zero angle was 1.8×10^{-6} cm^2•s^{-1}, almost 4 times lower than that of the fast mode of $C_{12}C_{12}C_{12}$(Et) under the same conditions, even though the molecular mass of DTEAB is at least 2 times smaller.

Figure 5 shows the changes in the fast and slow modes of $C_{12}C_{12}C_{12}$(Et) after adding NaBr into the solution. With increasing salt concentration, the size of the fast mode was increased and its distribution was also narrowed, while the amplitude of the

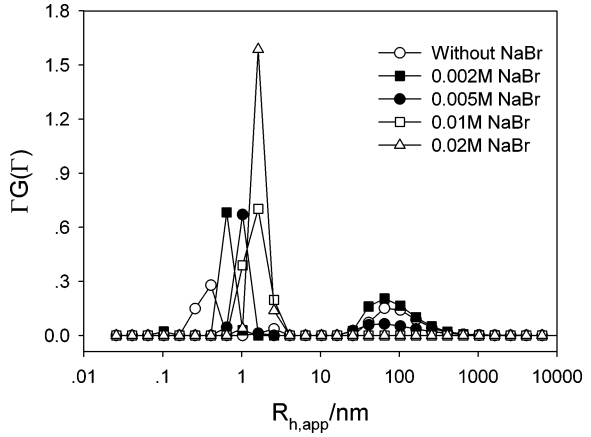

Figure 5. Salt effect on the bimodal distribution of $C_{12}C_{12}C_{12}$(Et) solution at 30°, $C = 5$ mM.

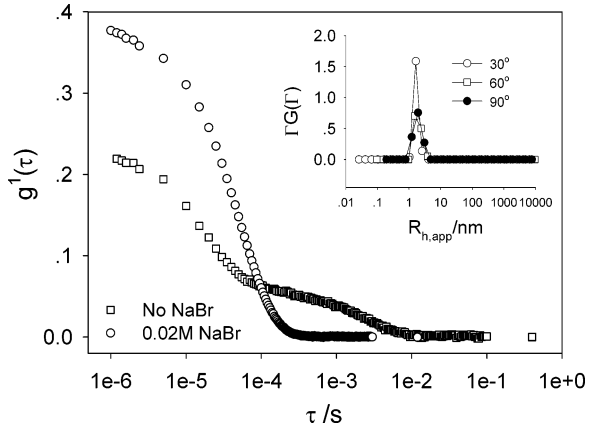

Figure 6. Normalized photon correlation curves of $C_{12}C_{12}C_{12}$(Et) solution with 0 and 0.02 M NaBr. The inset shows the CONTIN results with 0.02 M NaBr.

slow mode was sharply decreased without profound changes in size and size distribution. The fast mode lost its angular dependence at 0.002 M NaBr (data not shown), and the slow mode completely disappeared when the NaBr concentration reached 0.01 M. Figure 6 compares the normalized photon correlation function ($g^1(\tau)$) of $C_{12}C_{12}C_{12}$(Et) with 0 and 0.02 M NaBr measured at 30°. Note that the measured and calculated baselines have a difference below 0.1%. Due to the existence of the slow mode, two decays were detected in the correction curve with zero salt concentration, while single relaxation with higher apparent coherence was observed at 0.02 M NaBr. The inset in Figure 6 also indicates that the $R_{h,app}$ of the component formed by $C_{12}C_{12}C_{12}$(Et) at 0.02 M NaBr was about 1.8 nm and showed no angular dependence.

Figure 7 shows the photon correlation functions of DTEAB with and without NaBr. At higher salt concentrations, the correlation curve of DTEAB was almost the same as that of $C_{12}C_{12}C_{12}$(Et), and so was the size distribution after CONTIN analysis (inset in Figure 7). Figure 7 also shows that the slow decay in the correlation curve of DTEAB without salt is barely visible, which is quite different from that of $C_{12}C_{12}C_{12}$(Et). Another major difference between DTEAB and $C_{12}C_{12}C_{12}$(Et) was their sensitivity to the salt concentration. As shown in Figure 8, the $R_{h,app}$ of $C_{12}C_{12}C_{12}$(Et) was increased from 0.35 nm at zero NaBr concentration to 1.8 nm at 0.02 M NaBr, which corresponds to an increase by a factor of 5, while the size of DTEAB was only slightly increased by a factor of 1.4 (from 1.33 to 1.9 nm) over a similar salt to surfactant molar ratio range. The inset in Figure 8 shows that the absolute excess intensity increases with

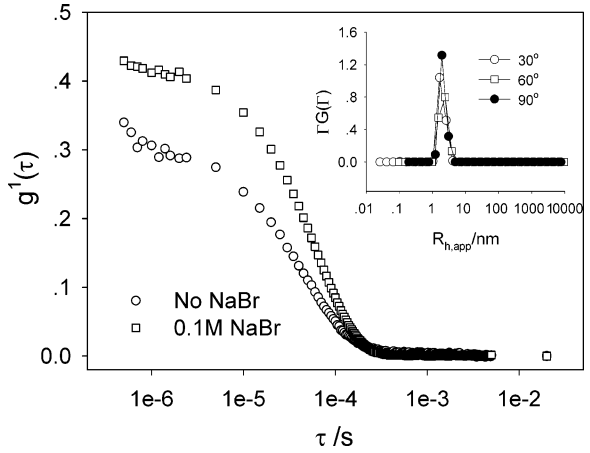

Figure 7. Normalized photon correlation curves of DTEAB solution with 0 and 0.1 M NaBr. The inset shows the CONTIN results with 0.1 M NaBr.

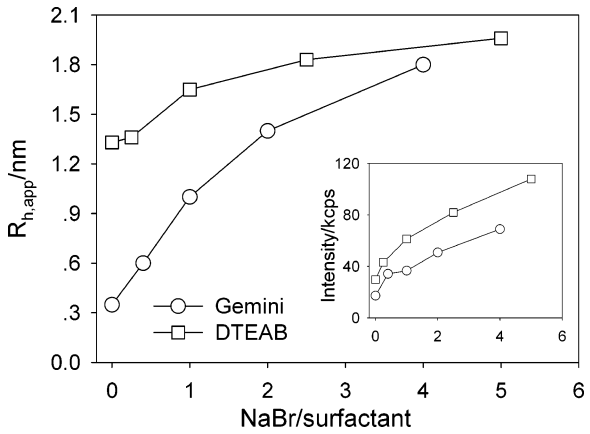

Figure 8. Changes in $R_{h,app}$ and excess scattered intensity (inset) of $C_{12}C_{12}C_{12}$(Et) and DTEAB at varying NaBr to surfactant ratio.

increasing NaBr concentration both in DTEAB and $C_{12}C_{12}C_{12}$-(Et). From the theory of laser light scattering, the scattered intensity was roughly proportional to sixth power of the particle size. Even though the slow mode in $C_{12}C_{12}C_{12}$(Et) solution with zero NaBr concentration was 87 nm (Figure 1), ~40 times larger than that (1.8 nm) of $C_{12}C_{12}C_{12}$(Et) with 0.02 M NaBr, its excess scattered intensity (17.2 Kcps) was 4 times lower, indicating that the excess scattered intensity was mainly contributed by the fast mode instead of the slow mode. According to eq 1, the $G(\Gamma)$ value obtained from CONTIN was directly related to the scattered intensity. Even though the size of the fast mode was 2 orders smaller, its peak area was larger than that of the slow mode at almost all the scattering angles (Figure 1), indicating that $C_{12}C_{12}C_{12}$(Et) molecules in the slow mode were scarce. Low density due to loose packing was another possible reason that the slow mode generated less scattered intensity.

Based on the above discussions, the "extraordinary regime" did exist in $C_{12}C_{12}C_{12}$(Et) solution at low salt concentrations. TEM experiments have demonstrated the formation of vesicles by $C_{12}C_{12}C_{12}$(Et) at zero salt concentration.[2] With the aid of freeze fracture techniques, vesicles with diameters ranging from 20 to 60 nm were visualized in the microscope. The size observed in TEM was much smaller than that measured by DLS, where the average diameter was about 170 nm. Such big difference could not be caused by freezing when performing TEM. Therefore, the two modes observed in Figure 1 resulted from neither the diffusion of the individual surfactant molecules nor that of the aggregates observed in TEM. In brief, the gemini

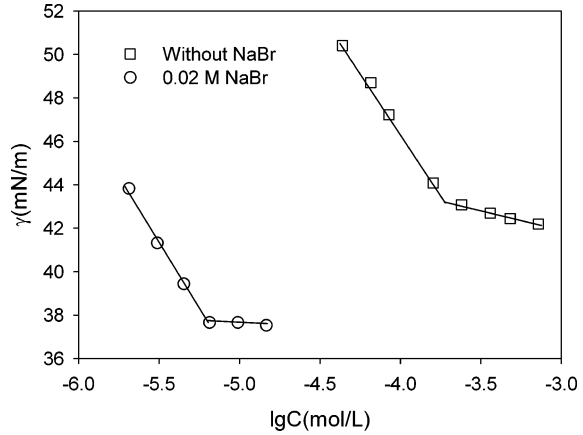

Figure 9. Surface tension (γ) versus log C of $C_{12}C_{12}C_{12}$(Et) with and without 0.02 M NaBr.

surfactant followed similar rules as in the case of polyelectrolytes in aqueous solution when studied by DLS.

Figure 9 shows the changes in surface tension (γ) of water at varying $C_{12}C_{12}C_{12}$(Et) concentrations. Without salt, $C_{12}C_{12}C_{12}$-(Et) yielded a cmc value of 0.20 mM, about 30 times higher than that (0.0064 mM) after adding 0.02 M NaBr. Moreover, the efficiency in reducing the surface tension without salt was much lower, indicating that the packing of the surfactant molecules in the micellar structures at zero salt concentration was not as tight as that in the micelles formed in the presence of salt. Without effective shielding by salt, the two charges in $C_{12}C_{12}C_{12}$(Et) repelled each other to a certain distance to equilibrate with the shrinking force of the spacer and the side chains. Therefore, each $C_{12}C_{12}C_{12}$(Et) took a volume larger than double that of the monomeric surfactants, although their spacers adopted a folded wicket-like conformation. On the other hand, the electrostatic repulsions also kept the surfactant molecules away from each other. Therefore, $C_{12}C_{12}C_{12}$(Et) molecules had the tendency to stay individual, yielding a much higher cmc value. At a concentration above the cmc (5 mM in our studies), $C_{12}C_{12}C_{12}$-(Et) molecules formed micellar structures by loose packing or with a smaller aggregation number. According to the coupled-mode theory, the electric field generated by the mobile counterions imposed an accelerating force on the micellar structures at the thermal diffusing state, generating the fast mode with high diffusing speed and strong angular dependence (Figures 1 and 2). Working as macroions at zero salt concentration, the micellar structures were subject to forming multimacroion domains,[24,25] which are presented as the slow mode shown in Figure 1. The micrograph from TEM revealed vesicle structures after freeze fracture, indicating that ordered structures may already be present in the multimacroion domains.[2] An increase in concentration or temperature would enhance or weaken both the hydrophobic interaction and the electrostatic interaction, yielding less effect on the bimodal distribution as demonstrated in Figure 3.

When NaBr was added to screen the effective charges in the headgroup, the electrostatic repulsion was weakened and its working range was also shortened, making the hydrophobic interactions relatively stronger. On one hand, the slow mode completely disappeared when the NaBr concentration reached 0.01 M, indicating that the multimacroion domains have been destroyed by NaBr. On the other hand, the increase in the salt concentration gradually decoupled the dynamics of the micellar structure and the counterions, resulting in the increase in $R_{h,app}$.

(24) Sedlák, M. *J. Chem. Phys* **2002**, *116* (12), 5256.
(25) Sedlák, M. *J. Chem. Phys.* **2005**, *122* (15), 151102/1.

A close packing between the surfactant molecules and an increase in aggregation number due to the screening of the electrostatic repulsion also led to an increase in $R_{h,app}$ and in excess scattered intensity (Figure 8). With further increasing salt concentration to decrease the range and strength of the electrostatic repulsion, $C_{12}C_{12}C_{12}$(Et) molecules just behaved like regular amphiphilic surfactants. They self-assembled into micellar structures with the side chains and spacers forming the core and the headgroups forming the corona. The molecular density in the micelle should be much higher than that of the multimacroion domains formed at zero salt concentration, because of the enhanced hydrophobic attraction or the reduced electrostatic repulsion.

As discussed above, it was the strong electrostatic interaction that controlled the "extraordinary regime" of $C_{12}C_{12}C_{12}$(Et) in aqueous solution without added salt. The hydrophobic interaction drove the surfactants to form micelle structures when the electrostatic interaction was effectively screened. In other words, the "extraordinary regime" would be sharply reduced if the electrostatic interaction was much weaker than the hydrophobic attraction. It was the case as demonstrated by DTEAB. With only one charge in the headgroup, the electrostatic interaction between DTEAB molecules was only 1/4 of that of $C_{12}C_{12}C_{12}$-(Et) molecules according to Coulomb's law. Therefore, no prominent "extraordinary" behavior was observed for DTEAB at zero salt concentration (Figures 4 and 7). Instead, aggregation of DTEAB was evidenced by the $R_{h,app}$ value, where single DTEAB molecules could not be as large as 2.66 nm in diameter (Figure 8). Adding NaBr merely enhanced the aggregation process due to the charge screening.

Conclusions

Similar to the case of polyelectrolytes, an "extraordinary regime" was observed in $C_{12}C_{12}C_{12}$(Et) solutions at low salt concentration. Due to the strong electrostatic interactions, a characteristic bimodal distribution, with none of the modes representing the correct diffusion value of a single surfactant or the micellar structures, was observed by DLS at all the scattering angles. The fast mode was reasonably explained by the coupled-mode theory, and the slow mode could be interpreted as the multimacroion domains. When adding NaBr to screen the effective charge, the slow mode was quickly eliminated, and a decoupling between the micellar structures and the counterions was also observed.

Acknowledgment. Financial support of this work by the Chinese National Science Foundation (20504001, 20425310, 20633010) and National Basic Research Program of China (Grant No. 2007CB936201) is gratefully acknowledged.

LA702832V